

## Hadronization via Coalescence

V. Greco<sup>1</sup> and C.M. Ko<sup>1</sup>

<sup>1</sup> Cyclotron Institute and Physics Department, Texas A&M University,  
TX-77843-3366 College Station, USA

**Abstract.** We review the quark coalescence model for hadronization in relativistic heavy ion collisions and show how it can explain the observed large baryon to meson ratio at intermediate transverse momentum and scaling of the elliptic flows of identified hadrons. We also show its predictions on higher-order anisotropic flows and discuss how quark coalescence applied to open- and hidden-charm mesons can give insight to charm quark interactions in the quark-gluon plasma and  $J/\Psi$  production in heavy ion collisions.

*Keywords:* quark coalescence,  $\bar{p}/\pi$  ratio, elliptic flow,  $J/\psi$ , and D meson  
*PACS:* 25.75.Dw, 25.75.Nq, 12.38Bx

### 1. Introduction

To find the signals of the quark-gluon plasma and to study its properties in relativistic heavy ion collisions, it is important to understand how quarks and gluons are converted to hadrons during hadronization. Because of its non-perturbative nature, hadronization has so far been treated only phenomenologically based on the statistical model, the duality model, or the coalescence model. The coalescence model, in which colored partons are combined into singlet hadron clusters, was first suggested as a possible mechanism of hadronization in studying pion correlations in relativistic heavy ion collisions [ 1]. It was later applied to describe the chemical composition of the hadronic matter produced in heavy ion collisions at SPS and RHIC [ 2]. More recently, the quark coalescence model has been shown to explain not only the larger baryon to pion ratio at intermediate transverse momentum but also the scaling relation among the elliptic flows of identified hadrons that are observed in Au+Au collisions at the Relativistic Heavy Ion Collider (RHIC) [ 3, 4, 5, 6, 7, 8]. In this talk, the quark coalescence model and its applications to heavy ion collisions at RHIC will be reviewed. Besides particle spectra and elliptic flows, we also discuss results from the coalescence model on resonance production, higher-order  $v_4$  flow, and charmed hadron production and flow.

## 2. The coalescence model

In the coalescence model, the transverse momentum spectrum of hadrons that consist of  $n$  quarks is given by the overlap of the product of  $n$  quark phase-space distribution function  $f_q(x_i, p_i)$  with the Wigner distribution function  $f_H(x_1..x_n; p_1..p_n)$  of the hadron, multiplied by the probability  $g_H$  of forming from  $n$  colored quarks a color neutral object with the spin and isospin of the hadron, i.e.,

$$\frac{dN_H}{d^2P_T} = g_H \int \prod_{i=1}^n \frac{p_i \cdot d\sigma_i d^3\mathbf{p}_i}{(2\pi)^3 E_i} f_q(x_i, p_i) f_H(x_1..x_n; p_1..p_n) \delta^{(2)}\left(P_T - \sum_{i=1}^n p_{T,i}\right), \quad (1)$$

where  $d\sigma$  denotes an element of a space-like hypersurface.

The  $n$  quark phase space distribution is usually approximated by the product of the single quark distribution function, which consists of both a thermal and a minijet component, separated by the transverse momentum  $p_0 \sim 2$  GeV. For heavy ion collisions at RHIC, the quark transverse momentum spectrum below  $p_0$  is taken to be thermal with a temperature  $T = 170$  MeV and a radial flow velocity  $\beta = 0.5$ , which are consistent with both experimental data and predictions from hydrodynamical calculations. The masses of thermal quarks are taken to be those of constituent quarks, i.e.,  $m_{u,d} = 300$  MeV and  $m_s = 475$  MeV. Above  $p_0$ , partons are from the quenched pQCD minijets with power-law like transverse momentum spectrum [ 9], and their masses are those of current quarks. Both soft thermal and hard minijet partons are assumed to distribute uniformly in a fireball of transverse radius of 8.15 fm and longitudinal length of 4.35 fm, corresponding to a volume of 900 fm<sup>3</sup>. The number of quarks are then fixed by the measured transverse energy of about 700 GeV for Au+Au collisions at  $\sqrt{s_{NN}} = 200$  GeV.

For the Wigner distribution functions of hadrons, they are taken to be a sphere in both space and momentum with radii  $\Delta_r$  and  $\Delta_p$ , respectively, which are further related by  $\Delta_r \cdot \Delta_p^{-1} = 1$  according to the uncertainty principle. A good description of both pion and proton spectra can be obtained with a radius parameter of  $\Delta_p = 0.24$  GeV for mesons and 0.35 GeV for baryons.

## 3. Particle spectra and elliptic flows

In coalescence model, hadrons are formed from quarks that are close in phase space. As a result, baryons with momentum  $p_T$  are produced from quarks with momenta  $\sim p_T/3$ , while mesons with same momentum are from quarks with momenta  $\sim p_T/2$ . Since the transverse momentum spectra of quarks decrease with  $p_T$ , production of high momentum baryons from quark coalescence is more favored than mesons. This is opposite to the fragmentation process where baryon production is penalized with respect to mesons as more quarks need to be produced from the vacuum, leading to a typical  $p/\pi$  ratio of  $\sim 0.2$ . Results on  $\bar{p}/\pi$  ratio based on Eq.(1) are shown in Fig.1(left) together with data from PHENIX [ 10]. Although different methods have been used in evaluating the coalescence integral in Eq.(1) (for a review see [

11)), they all lead to enhanced  $\bar{p}/\pi$  ratio (and similarly the  $K/\Lambda$  ratio). As shown in Fig.1(left), our approach [ 5, 6], which includes resonance decays (to be described in the next paragraph) and avoids the collinear approximation by using the Monte Carlo method to evaluate the multi-dimensional coalescence integral, also gives a good description of the  $\bar{p}/\pi$  ratio at  $p_T < 2$  GeV.

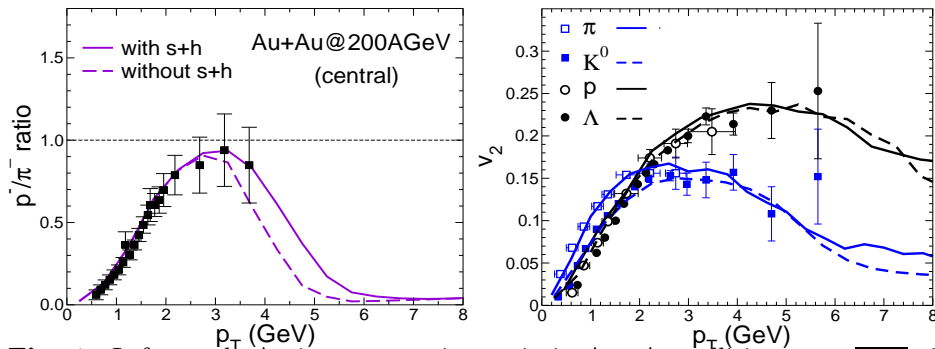


**Fig. 1.** Left panel: Antiproton to pion ratio in Au+Au collisions at  $\sqrt{s_{NN}}=200$  GeV. Solid and dashed curves are results with and without contribution to antiproton from coalescence of thermal with minijet partons. Filled squares are experimental data from PHENIX [ 10]. Right panel: Elliptic flows of identified hadrons. Lines are from the coalescence model, while symbols are data from STAR [ 13] and PHENIX [ 14].

Another typical feature of quark coalescence is the scaling of hadron elliptic flows according to the number of constituent quarks in a hadron:  $v_{2,H}(p_T)/n = v_{2,q}(p_T/n)$ , which can be derived under the approximation that only quarks with equal momentum can coalesce into hadrons [ 8]. Without any constraint on the relative momentum of coalescing quarks, the scaling relation between baryon and meson elliptic flows can be badly violated [ 12]. In our coalescence model, we have taken into account the finite momentum distribution of quarks inside hadrons, and this leads to only a small breaking ( $\sim 5\%$ ) of the so-called “coalescence scaling” [ 6], which is seen to hold within the errors of experimental data [ 13, 14].

In Fig.1 (right), we show how the results from our coalescence model can reproduce the available experimental data [ 13, 14] for  $\pi, K, p, \Lambda$  once the quark elliptic flow is extracted from a fit to the pion data [ 6]. We note that the contribution of hadrons from minijet fragmentation is not included in this calculation. Its inclusion would lead to a universal hadron elliptic flow at momentum above  $p_T \sim 6$  GeV [ 7]. In Ref.[ 6], the quark elliptic flow was extracted from a fit to the pion data, and its shape, especially the saturation at  $p_T \sim 1$  GeV, is in agreement with that from parton cascade calculations [ 15]. At low momenta, the elliptic flow from the hydrodynamical model at the phase transition temperature could also be used in the coalescence model calculations for hadron elliptic flows. This is because the description of elliptic flows at low  $p_T$  are similar in the hydrodynamical and the coalescence model, once we correct for energy conservation in quark coalescence

and include the residual radial flow effect from the hadronic stage.

Another possible source of scaling breaking in hadron elliptic flows is the feed-down from resonance decays. We have studied how elliptic flow of stable hadrons are affected by contributions from the decay of resonances [ 16]. Particles from these decays have in principle a different elliptic flow from that of resonances, and its value depends on the competition between a shift in their momenta, which gives a larger elliptic flow, and the randomization of their momenta, that decreases their initial azimuthal anisotropy. It turns out that particles like  $p$ ,  $\Lambda$ , and  $K$  from resonance decays have elliptic flows that are very similar to the directly produced ones. Therefore, the inclusion of resonance effect does not destroy the coalescence scaling of these stable hadrons. On the other hand, pions from the decay of  $\omega$ ,  $K^*$ ,  $\Delta$  show a significant enhancement of their elliptic flow at  $p_T < 2$  GeV. Although, the effect of these resonances is reduced by pions from rho meson decays, which have an elliptic flow more close to that of direct pions, the overall effect of resonance decays on pion elliptic flow is still non-negligible. The breaking of coalescence scaling due to resonance decays together with that due to finite quark momentum spread mentioned above lead to a better agreement with available data as shown in Fig.1(left), where the decay of resonances was included [ 6, 16]. However, one should be aware that such an agreement may be fortuitous especially at very low  $p_T$ , again because of the lack of energy conservation in quark coalescence.

Higher-order momentum anisotropy have also be measured recently in experiments. In particular, the fourth-order harmonic  $v_4$  was found to be sizeable [ 17], as first suggested in Ref.[ 18]. Higher-order flows provide the possibility to further test the coalescence picture for hadronization. Based on the naive coalescence model that only allows quarks of equal momentum to form a hadron, it has been shown that the meson  $v_{4,M}$  and baryon  $v_{4,B}$  are related to quark  $v_{2,q}$  and  $v_{4,q}$  by [ 19]:

$$v_{4,M}(2p_T) \simeq 2v_{4,q} + v_{2,q}^2 \quad v_{4,B}(3p_T) \simeq 3v_{4,q} + 3v_{2,q}^2, \quad (2)$$

with  $v_{n,q}$ 's evaluated at  $p_T$ . We can see that the ratio between baryon and meson  $v_4$  is 3 if there is no  $v_{4,q}$  at quark level. However, a fit to the charged particle  $v_4$  data using the quark coalescence model requires that  $v_{4,q} \simeq 1.8v_{2,q}^2$ , which is similar to  $v_{4,q} \sim v_{2,q}^2$  from the parton cascade [ 15]. With non-zero  $v_{4,q}$ ,  $v_{4,B}/v_{4,M}$  is thus expected to be less than 3. These results are shown in Fig.2 (left) together with experimental data on  $v_4$  of charged hadrons.

#### 4. $J/\Psi$ and D meson

The coalescence model can also be used to study open and hidden charmed hadron production in relativistic heavy ion collisions. With the large heavy quark mass, a more rigorous treatment of the coalescence process can be achieved [ 20]. Study of charm meson production at RHIC using the quark coalescence model allows us to address the following issues: (a) What is the sensitivity of the  $J/\Psi$  abundance and its  $p_T$  spectrum to the momentum distribution of charm quarks? (b) How

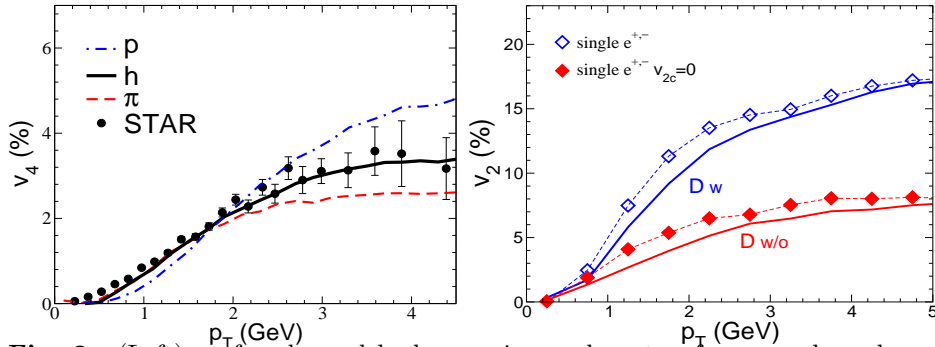


**Fig. 2.** (Left)  $v_4$  for charged hadrons, pion and proton from quark coalescence together with the experimental data (STAR) for charged hadrons [ 17]. (Right) Elliptic flow for D mesons and single electrons from their decays.

does the interplay of charm- and light-quark distributions translate into the elliptic flow of  $D$ -mesons? Without assuming complete thermalization of charm quark, which is common to statistical models, makes it possible to discriminate the relative importance between  $J/\psi$  regeneration and suppression in relativistic heavy ion collisions. Studies based on the rate equation have shown that regeneration of  $J/\Psi$  can bring its abundance back to the initial value expected from the superposition of nucleon-nucleon interactions [ 21]. On the other hand, the initial momentum distribution of charm quarks from the PYTHIA routines is much broader than if they are thermalized in the quark-gluon plasma. The average relative momentum between two quarks is thus larger than that of the charm quarks inside the charmonium. Quantitatively, this causes a decrease of their recombination probability into  $J/\Psi$  by about a factor 3 with respect to the thermal case [ 22].

Another way of probing charm interactions in the medium is through the elliptic flow of single electrons from  $D$  meson decays. We have already shown how quark coalescence is able to describe the elliptic flow of light hadrons. Our knowledge of  $v_2(p_T)$  for light hadrons thus allows for a quantitative prediction of  $v_{2D}(p_T)$  for the case in which charm quarks do not experience any final-state interactions. This represents the lower limit for the  $v_{2D}$  of  $D$  mesons (D w/o in Fig.2 (right)), because it is only due to the elliptic flow of light quarks. An upper limit can be obtained by assuming that charm quarks have a  $v_{2D}$  equal to that of light quark (D w in Fig.2(right)). It is also seen in Fig.2(right) that single electrons (diamonds) from  $D$  meson decays have essentially the same flow as that of  $D$  mesons.

In our calculations, we have not included  $D$  mesons produced from jet fragmentation. The elliptic flow of these  $D$  mesons depends on the energy loss of charm quarks in the quark-gluon plasma. Since the latter is predicted to be smaller than that of light quarks, a quite small  $v_2$  (a first estimation put the upper limit around 5% [ 23]) is expected from these  $D$  mesons. Experimental measurement of  $v_{2D}$  thus allows to distinguish between the quark coalescence and the jet fragmentation mechanism for  $D$  meson production in relativistic heavy ion collisions.

## Acknowledgments

We thank our collaborators, L.W. Chen, P. Lévai, P. Kolb, and R. Rapp, during different phases of the presented work. This talk was based on work supported in part by the US National Science Foundation under Grant No. PHY-0098805 and the Welch Foundation under Grant No. A-1358. VG was further supported by the National Institute of Nuclear Physics (INFN) in Italy.

## References

1. J.A. Lopez, J.C. Parikh, and P.J. Siemens, Phys. Rev. Lett. **53**, 1216 (1983).
2. T.S. Biró, P. Lévai, and J. Zimányi, Phys. Lett. B **347**, 6 (1995); J. Phys. G **28**, 1561 (2002).
3. S.A. Voloshin, Nucl. Phys. A **715**, 379 (2003).
4. R.C. Hwa and C.B. Yang, Phys. Rev. C **67**, 034902 (2003); 064902 (2003); Phys. Rev. Lett. **90**, 212301 (2003).
5. V. Greco, C.M. Ko, and P. Lévai, Phys. Rev. Lett. **90**, 202302 (2003).
6. V. Greco, C.M. Ko, and P. Lévai, Phys. Rev. C **68**, 034904 (2003).
7. R.J. Fries, B. Müller, C. Nonaka, and S.A. Bass, Phys. Rev. Lett. **90**, 202303 (2003); Phys. Rev. C **68**, 044902 (2003).
8. D. Molnar and S.A. Voloshin, Phys. Rev. Lett. **91**, 092301 (2003).
9. M. Gyulassy, P. Lévai, and I. Vitev, Phys. Lett. B **538**, 282 (2002).
10. S. Esumi, PHENIX Collaboration, Nucl. Phys. A **715**, 599 (2002).
11. R.J. Fries, Proceedings of Quark-Matter 2004, nucl-th/0403036.
12. Z.W. Lin and D. Molnar, Phys. Rev. C **68**, 044901 (2003).
13. P. Sorensen, J. Phys. G. **30**, S217 (2004); *and these proceedings*.
14. J. Velkovska, *these proceedings*.
15. L.W. Chen, C.M. Ko, and Z.W. Lin, Phys. Rev. C **69**, 031901 (2004).
16. V. Greco and C.M. Ko, nucl-th/0402020.
17. J. Adams *et al.*, STAR Collaboration, nucl-ex/0310029.
18. P.F. Kolb, Phys. Rev. C **68**, 031902(R) (2003).
19. P. Kolb, L.W. Chen, V. Greco, and C. M. Ko, Phys. Rev. C, in press; nucl-th/0402049.
20. E. Braaten, Y. Jia, and T. Mehen, Phys. Rev. Lett. **89**, 122002 (2002).
21. L. Grandchamp and R. Rapp, Phys. Lett. B **523**, 60 (2001); Nucl. Phys. **A709**, 415 (2002).
22. V. Greco, C.M. Ko, and R. Rapp, nucl-th/0312100.
23. M. Djordjevic and M. Gyulassy, Phys. Lett. B **560**, 37 (2003); *and these proceedings*.